24th COBEM - 2017

24[th] ABCM International Congress of Mechanical Engineering
December 3-8, 2017, Curitiba, PR, Brazil

COBEM-2017-0716
SIMULATION OF MACRO-EMULSION FLOW IN STRATIFIED RESERVOIRS CONSIDERING CAPILLARY EFFECTS

Ranena V. Ponce F.
Helena Lima
Márcio S. Carvalho
Pontificia Universidade Católica do Rio de Janeiro
poncerv@puc-rio.br, msc@puc-rio.br

Abstract. *Oil-water emulsion injection has shown significant potential as Enhanced Oil Recovery (EOR) method. Experimental results showed that droplet size, drop concentration and local capillary number as the most relevant parameters affecting emulsion performance as water phase mobility control agent. Emulsion injection and production predictions in real reservoirs requires deep understanding of their flow at pore scale and the underlying mechanisms responsible for the macroscopic improved oil recovery. Ponce* et al. *(2017) developed a macroscopic model to represent emulsions flow in porous media by relative permeability curves parametrization as function of emulsion concentration and local capillary number. In this work, gravitational effects were incorporated into the model in order to evaluate vertical sweep efficiency of water alternating emulsion injection (WAE) in highly heterogeneous reservoirs. Parametric analysis on time for emulsion injection, emulsion bank size and local capillary number was performed in 2D and 3D simulations models to explore WAE performance. Results showed that extra oil recoveries higher than waterflooding may be reached even with reduced emulsion bank size. Oil production acceleration was observed under WAE processes with early emulsion injection. 3D simulations results showed the significant potential of emulsions to enhance vertical sweep efficiency in stratified reservoirs.*

Keywords: *Emulsion, Enhanced Oil Recovery, Mobility Control, Reservoir Simulation*

1. INTRODUCTION

Water injection is the most widely method used for oil recovery worldwide, however, unfavourable mobility ratio between the displacing and displaced fluid, as well as reservoir heterogeneities, are factors that promotes channeling of the injected water which results in an overall low sweep efficiency during oil displacement.

Several studies have shown the significant potential of oil-in-water emulsion injection to overcome this issues and increase oil recovery. After a series of successful crude oil-in-water emulsion injection experiments on sandstones, McAuliffe (1973) conducted field tests in the Midway-Sunset field (USA) obtaining a substantial oil recovery gain. Production records showed water cut reduction in monitored wells, indicating that emulsion efficiently blocked zones with high degree of viscous fingering. Also, flow path changes were confirmed by tracers detection in producers wells previously not reached during waterflooding, and evidence of an increased oil sweep efficiency was supported by records of increased water salinity.

During WAE injection in a sand packed porous media Guillen *et al.* (2012a) visualized at pore-level an improvement on displacement efficiency by recording the mobilization of oil initially by-passed by water. Also, the emulsion mobility control potential at macroscale was observed in experiments on parallel sandstone cores with different permeabilities. Simultaneous WAE injection on both cores resulted in extra oil recovery from the high permeability sandstone, while oil production only occurs in the lower permeability core after emulsion injection.

Guillen *et al.* (2012b) observed that the emulsion mobility control effectiveness is a strong function of capillary number. A similar behavior was noted by Romero *et al.* (2011), who found out during WAE tests in cores, that the lower the capillary number the more effective the mobility control and that a critical value may be estimated to maximize emulsion performance.

Coreflood test made in sandstones to determine oil-emulsion (O/E) relative permeability (Kr) curves with different drop size distributions were conducted by Engelke *et al.* (2013). Results showed a significant reduction on residual oil saturation and water-phase relative permeability end-point when compared with oil-water (O/W) Kr curves, being this effect more pronounced for the larger drop size distribution. Moreover, reservoir simulations with experimental Kr curves showed that emulsions could delay water breakthrough and increase oil recovery.

It is well known that heterogeneities in reservoirs impact fluid flow of any production strategy, and emulsion injection arises as an EOR method that may enhance production scenarios in stratified reservoirs. However, to predict the benefits of emulsion injection in reservoir flow simulations, is necessary to understand their flow in porous media in order to propose models that upscale the mechanisms responsible for oil recovery improvement from pore-to-macroscopic level.

Recently, Ponce *et al.* (2014, 2017) developed a macroscopic model for emulsion flow in porous media by parametrizing relative permeability curves as function of emulsion drop concentration and local capillary number. In order to study emulsion benefits in stratified reservoirs, in this work the last model was upgraded by adding gravitational effects.

2. SIMULATION MODEL

Ponce *et al.* (2014) parametrized the water phase relative permeability curves as function of emulsion dispersed phase concentration. In the model, water mobility control and displacement sweep efficiency mechanisms, aim to describe the blockage of previously waterflooded reservoir zones and diversion of the water front to the unswept areas during the WAE flow, which in turns produce trapped oil. In their description, they model the flow of diluted stable o/w emulsions in porous media, flow is said to be incompressible and transport of the dispersed drops are purely convective as well as isothermal.

Experimental observations by Cobos *et al.* (2009) and Guillen *et al.* (2012b) revealed that emulsion flow in porous media is governed by capillary number (Ca), which is given by:

$$Ca = \frac{\mu \upsilon}{\sigma} \tag{1}$$

where μ is the viscosity of the displacing fluid, υ is the Darcy velocity, and σ the interfacial tension. The authors found out that there is a range of capillary number where viscous and capillary forces competes for mobilization/retention of the drops in the pore throats which is ruled locally by two critical capillary numbers: Ca_{min}, which is the minimum capillary number below which emulsion drops blocks continuously, and Ca_{max}, the maximum capillary number above which drops deforms and emulsion behave as water. Based in these observations, the initial model was subsequently altered in Ponce *et al.* (2017) to add dependency of the water phase Kr curves on capillary number.

To properly implement this dependency, a two phase black-oil model developed in the open source MRST by Aarnes *et al.* (2007) was modified. Emulsion transport equation and the water phase Kr curves parametrization as function of the local capillary number and the emulsion dispersed phase concentration (C_e) were added into the model. Parametrization was made in two interpolation steps. First, linear interpolations between the O/W and O/E systems are made as function of the local capillary number to calculate residual oil saturations, Corey's exponents and water phase end-points. In a second stage, these parameters were recalculated as a function of the emulsion concentration by interpolations between the calculated parameters in the first step and those of the water phase. With the recalculated parameters oil-emulsion Kr curves are calculated by using Corey (1954) correlations. Details of the interpolation process may be found in Ponce *et al.* (2017). To add gravitational forces into the model, the system of equations used in Ponce *et al.* (2017) were changed accordingly. The emulsion transport equation was modified to:

$$\phi \frac{\partial \left(C_e S_w\right)}{\partial t} + \nabla \cdot \left\{Cef_w \left[\upsilon - \mathbf{K}\lambda_o \left(\rho_w - \rho_o\right) g \nabla z\right]\right\} = C_e^0 \left(\frac{q_w}{\rho_w}\right) + C_e f_w q \tag{2}$$

In the same fashion were obtained the pressure (3) and saturation (4) equations

$$-\nabla \cdot \left[\mathbf{K}\lambda \nabla p + \mathbf{K}\left(\lambda_w \rho_w + \lambda_o \rho_o\right) g \nabla z\right] = q \tag{3}$$

$$\phi \frac{\partial S_w}{\partial t} + \nabla \cdot \left\{f_w \left[\upsilon - \mathbf{K}\lambda_o \left(\rho_w - \rho_o\right) g \nabla z\right]\right\} = \frac{q_w}{\rho_w} \tag{4}$$

In the above equations S_w is the water saturation, f_w the fractional flow, $\mathbf{K}$ the absolute permeability tensor, ρ_o and ρ_w the oil and water densities, C_e^0 the injected emulsion dispersed drop concentration, q and q_w the total and water phase flow rate, g the gravitational acceleration, t the time and z the distance in z-coordinate.

To solve the differential system of equations (2)-(4) boundary and initial conditions were defined. Consider a reservoir modeled in a cartesian grid with domain Ω and boundary $\partial\Omega$, injection and producer wells located at opposite corners with domains $\partial\Omega_i$ and $\partial\Omega_p$ respectively. Assuming non-slip conditions, prescribed producer pressure and injection flow rate (Q), and known irreducible water saturation (S_{wi}), the boundary and initial conditions are given by:

$$\mathbf{K}\lambda \nabla p \left(\partial\Omega, t\right) \cdot \vec{n} = 0 \tag{5}$$

$$p\left(\partial\Omega_p, t\right) = 0 \tag{6}$$

$$\frac{q_w}{\rho_w}\left(\partial\Omega_i, t\right) = Q \tag{7}$$

$$S_w\left(\Omega, 0\right) = S_{wi} \tag{8}$$

The differential system of equations (2)-(8) were discretized by the finite-volume method and partially decoupled in time step by using the IMPES method (*Implicit Pressure and Explicit Saturation*). With values of initial saturation distribution, the phases mobilities (λ_w, λ_o) are first calculated to solve Eq. (3) for pressure (p), which allows to compute total velocity field (υ). Then keeping υ constant, new mobilities, saturations and emulsion dispersed phase concentrations are calculated explicitly by solving iteratively Eqn. (2) and Eqn. (4).

3. RESULTS AND DISCUSSION

In order to study WAE performance and vertical sweep efficiency, the second model of the 10^{th} SPE Comparative Solution Project (Society of Petroleum Engineering, 2009) was used due to their high level of heterogeneity. The top part of the model is a *Tarbert* formation (near shore environment) while the lower part is fluvial (*Upper Ness* formation) . 2D simulations were performed in the first layer of the original grid (60 x 220 x 85 cells) while for 3D simulations 4 layers of an eighth of original reservoir area was used (30 x 55 x 4 cells).

According to Alvarado and Marsden (1979) emulsions with dispersed phase concentration lower than 50 vol% behave as newtonian fluid as the viscosity not differ too much from the water phase. Since we are modeling the flow of diluted emulsions, we selected a low emulsion concentration and assumed the same viscosity for water and emulsion (μ_w = μ_e = 0.001 Pa.s). Tables 1 and 2 show fluid properties as well as Corey's parameters used in the model, which calculates the relative permeability curves as function of the irreducible water saturation (S_{wi}), the residual oil saturation (S_{orw}), the oil and water phase relative permeabilities end-points (Kr_{owi},Kr_{wor}) and the Corey's exponents (n_o, n_w).

Table 1: Fluid properties.

Oil-water viscosity ratio, μ_o/μ_w	10
Interfacial tension, σ (mN/m)	24
Injected emulsion concentration, C_e^0 (vol %)	1
Water density, ρ_w (Kg/m^3)	997.7
Oil density, ρ_o (Kg/m^3)	994.92

Table 2: Corey's parameters for relative permeabilities calculation.

System	S_{wi}	S_{orw}	Kr_{owi}	Kr_{wor}	n_o	n_w
Oil-water	0.2	0.4	1	0.6	2	4
Oil-emulsion	0.2	0.2	1	0.2	2	4

Injector and producer wells were configured in a $1/4$ of five-spot scheme with completion in all layers along their domain. Flow rates were calculated for the 2D and 3D models by weighting the original flow rate of the SPE 10^{th} model by the volume of the cutout selected in each simulation. Wells were operated at constant flow rate for the injector and atmospheric bottom-hole pressure for the producer. WAE performance was studied by parametric analysis against waterflooding by comparing oil recovery factor (ORF), water-cut (WCUT) and injector bottom-hole pressure (IBP) as function of pore volume (PV). Oil saturation and cross sections maps are shown in 3D simulations to investigate vertical displacement efficiency.

3.1 2D SIMULATIONS

In all 2D simulations a total of 2.0 PV of fluids was injected at constant flow rate of $Q = 1.64{\times}10^{-4}$ m^3/s. Table 3 shows cases studied. Water injection (WI) is analyzed in case 1. All WAE injections was simulated by fixing a maximum capillary number of Ca_{max} = 4.47x10^{-6} for the emulsion model. Parametric analysis were performed on: Ca_{min} (to study the emulsion capillary number performance range), time for emulsion injection (or water pore volume injected before emulsion injection), and emulsion bank size (pore volume) injected.

Table 3: Studied cases of 2D simulations (1 layer).

Case	Process	Water injected before emulsion (PV)	Emulsion bank (PV)	Ca_{min}
1	WI	-	-	-
2				2.07×10^{-7}
3		0.3		4.47×10^{-8}
4			0.2	4.47×10^{-9}
5	WAE	0.1		
6				4.47×10^{-8}
7		0.2	0.1	
8			0.05	

First emulsion capillary number performance range were evaluated. Production results for cases 1-4 are presented in Fig. 1, in the graphs bank of emulsion is pointed by the green shaded area. In Figure 1(a) it is possible to note that the higher oil recovery (57.4%) is reached for the restricted range of capillary number for emulsion performance (Case 2), which is 14.4% higher than waterflooding. Reduction of Ca_{min} in order to increase the capillary number range for emulsion performance did not enhanced oil recovery reached in Case 2. This result highlights the importance of an appropriate emulsion design, which in order to get successful oil recovery it should be tailored to the reservoir rock features. The significant additional recovery obtained in Case 2 shows that there is an optimum capillary number range for emulsion performance where the reduction of water mobility and sweep efficiency can be maximized. The high bottom-hole injector pressure seen in Fig. 1(b) for Case 2 is related to the pore throats blockage by the emulsion drops and water invasion of unswept areas. Likewise, large oscillations observed in the WCUT may be associated to competition among viscous and capillary forces during displacement of the residual oil.

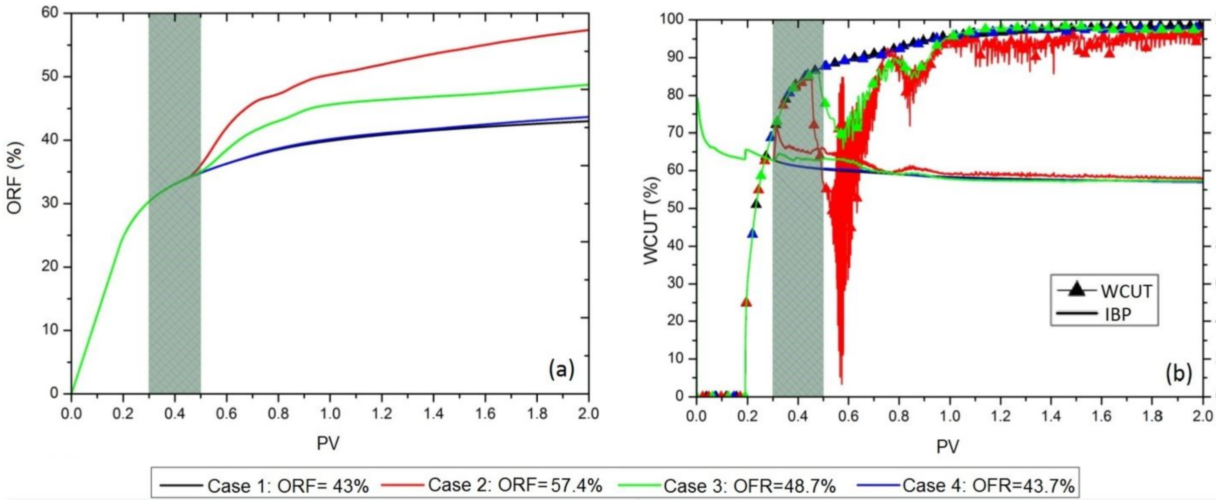

Figure 1: Effect of the emulsion capillary number performance range: Case 2 - restricted range (red line), Case 3 - medium range (green line) and Case 4 - wide range (blue line).

Effect of the time for emulsion injection is showed in Fig. 2. In this simulations Ca_{min} was fixed in 4.47 $\times10^{-8}$ and 0.2 PV of emulsion bank was injected after 0.3, 0.2 and 0.1 PV of water in Cases 3, 6 and 5 respectively.

Oil production acceleration can be seen in Figure 2(a) as the injection of the emulsion bench is anticipated. Although there is almost no difference between the ultimate ORF in the WAE cases, the worse of them (Case 3) recovered 5.7% more oil than continuous water injection. This results suggest that, even in heterogeneous reservoirs, anticipation of emulsion injection may enhance macroscopic mobility control of the injection front or flood conformance by suppressing early water breakthrough and mobilizing residual oil. The increase in the injector IBP and WCUT reduction observed in Fig 2(b) are consequence of the aforementioned changes in the flow pattern.

Effect of the emulsion bench size is shown in Fig. 3. After continuous water injection of 0.2 PV, injection of 0.05, 0.1 and 0.2 PV emulsion benchs were simulated in Cases 8, 7 and 6 respectively. It is possible to see in Fig 3(a) and (b) that the smaller the emulsion bench size the less oil recovery, water cut reduction and IBP. To limit the bench size reduces the effective area reached by emulsion, despite this, WAE cases simulated recovered among 4-6% more oil than waterflooding.

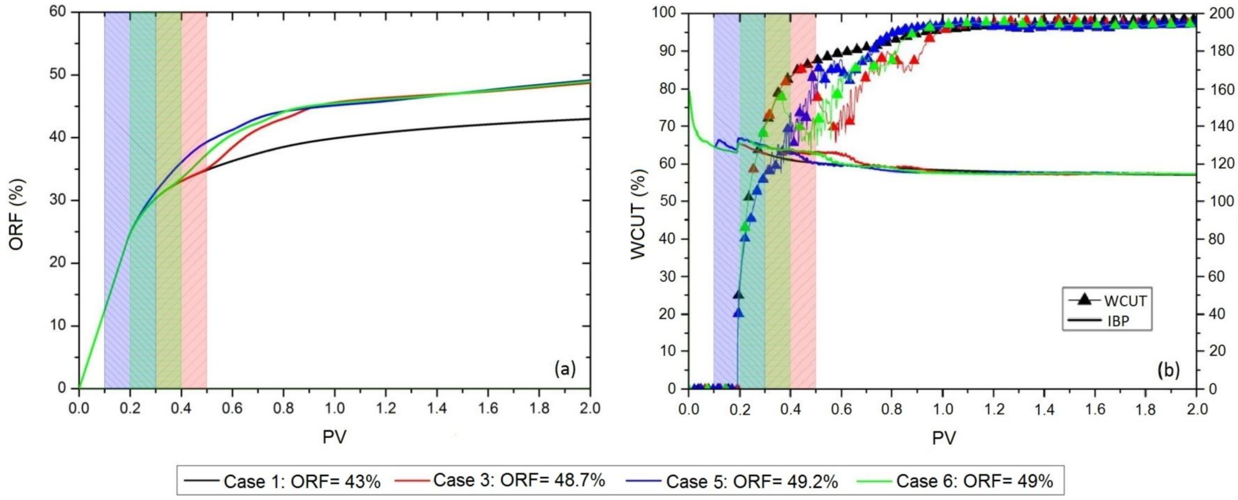

Figure 2: Effect of the time for emulsion injection. Emulsion bank was injected after: 0.3 (Case 3), 0.2 (Case 6) and 0.1 (Case 5) PV of water.

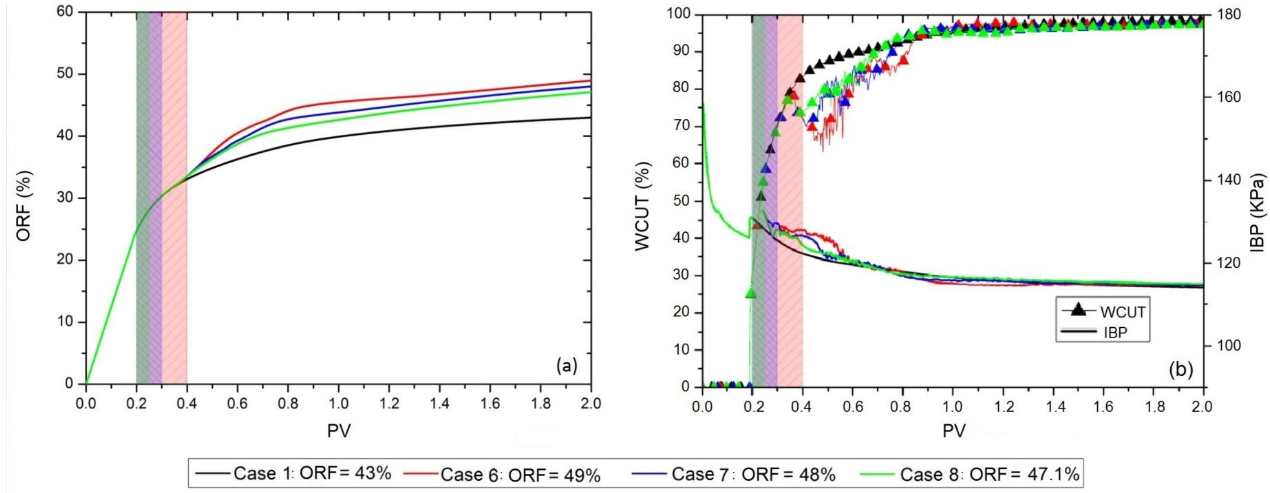

Figure 3: Effect of the injected emulsion bench size: 0.05 PV (Case 8), 0.1 (Case 6) and 0.2 (Case 7).

3.2 3D SIMULATIONS

In order to study the emulsion vertical displacement efficiency in stratified reservoirs, 4 layers from two locations of the geological model were selected: layers k=3-6 from the superior (*Tarbert*) formation and layers k=34-37 adjacent to both reservoir formations (*Tarbert* and *Upper Ness*). In both simulation models a total of 5 PV was injected at flow rate of $Q = 4.33\times10^{-4}$ m^3/s. WAE injection was simulated with values of Ca_{max}=2.5x10^{-6} and Ca_{min}=5x10^{-8} and parametric analysis was made on the time for emulsion injection and emulsion bench size. Table 4 shows cases studied in both simulation models.

Table 4: Cases studied in the 3D simulations models.

Process	Water injected before emulsion (PV)	Emulsion bank (PV)
WI	-	-
WAE	2.0	0.4
	0.2	
	0.4	
		0.2
		1.2

Figure 4(a)-(b) show, for both simulation models, the effect of the time for emulsion injection on production results.

ORF results shows for both simulation models that WAE injection recovery among 4.24 - 6.95% more oil than waterflooding. Similarly to the 2D simulations results, the sooner the emulsion bank is injected the more the oil production is accelerated. This behavior is more pronounced in the layers among both formations, which is accompanied by a large response in water cut and injector pressure as can be seen in Fig. 4(b). In order to understand this behavior oil saturation (So) maps were generated for water injection and the more efficient WAE process: (0.2/0.4/4.4)VP. Figures 5 and 6 show for both group of layers the absolute permeability maps and evolution of oil saturation along each injection process. In the figures the injector and producer wells are located in the lower left and the upper right corners respectively, and reduction in oil saturation in the frames is shown by colder colors.

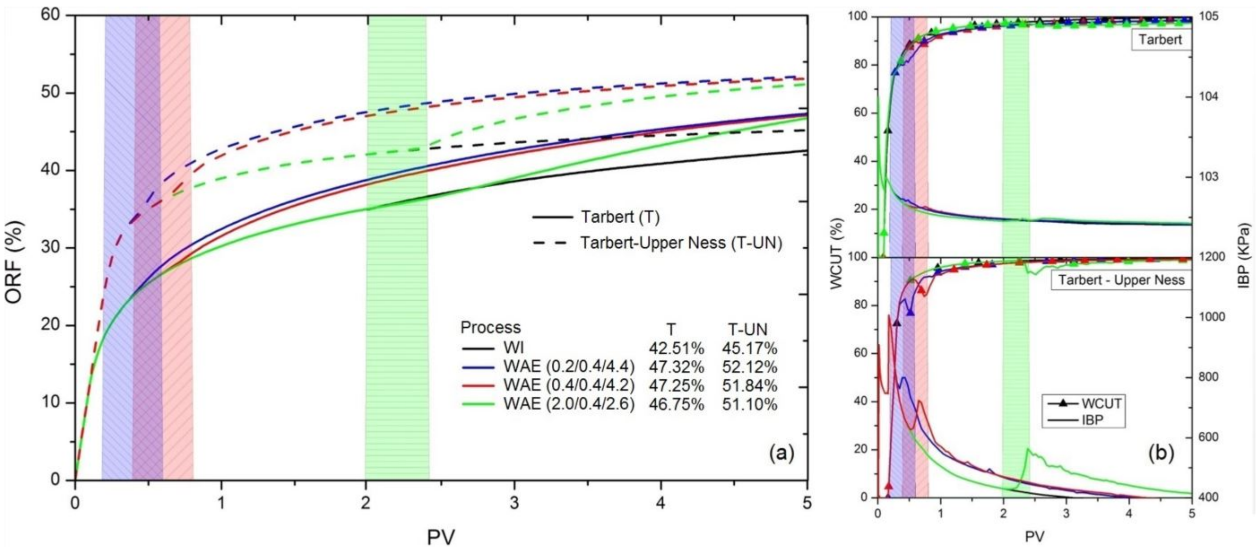

Figure 4: Effect of the time for emulsion injection in both group of layers.

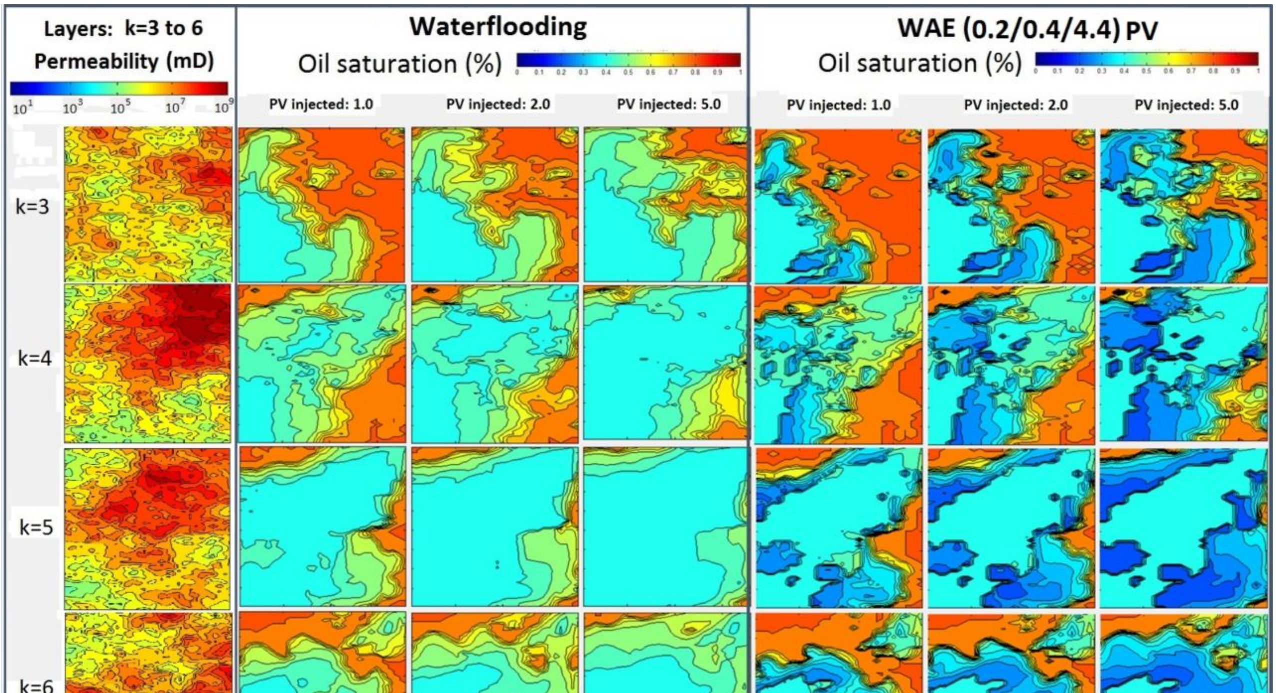

Figure 5: Absolute permeability map and evolution of oil saturation on layers k=3-6 (*Tarbert* formation) during waterflooding and WAE injection of (0.2/0.4/4.4) PV.

Comparing waterflooding results among layers of the same formation, it can be seen in Fig. 5 that differently than the lower layers, the first layer (k=3) has the worst sweep, situation that is improved in all layers with WAE injection. From Fig. 6 is possible to see a more uniform sweep during waterflooding, results that may be explained by the more

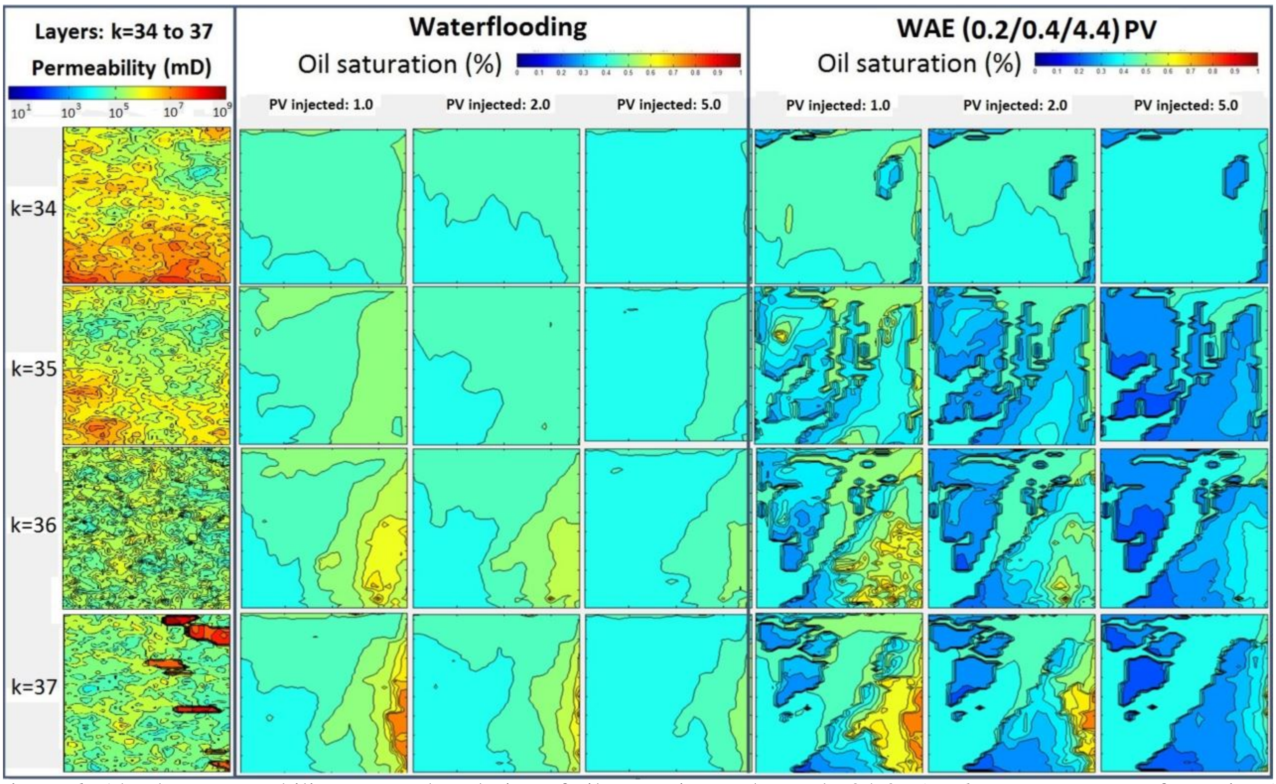

Figure 6: Absolute permeability map and evolution of oil saturation on layers k=34-37 (*Tarbert - Upper Ness* formations) during waterflooding and WAE injection of (0.2/0.4/4.4) PV.

homogeneous permeability distribution observed in all layers. It can be seen that oil sweep is enhanced in some areas of the layers after emulsion injection. Although water mobility control effect was not observed on saturation maps during WAE in none of the cases, displacement efficiency effect is marked in all layers of the model. In order to investigate vertical sweep efficiency after emulsion injection, oil saturation in cross sections of both simulation models were generated at constants (i,j) coordinates. Results for *Tarbert* and *Tarbert-Upper Ness* layers are shown in Fig. 7 and 8. By comparing both groups of layers at the same pore volume injected, a large difference can be observed in oil saturation due to the invasion of water after emulsion injection, this results evidence that vertical displacement efficiency is enhanced under WAE injection.

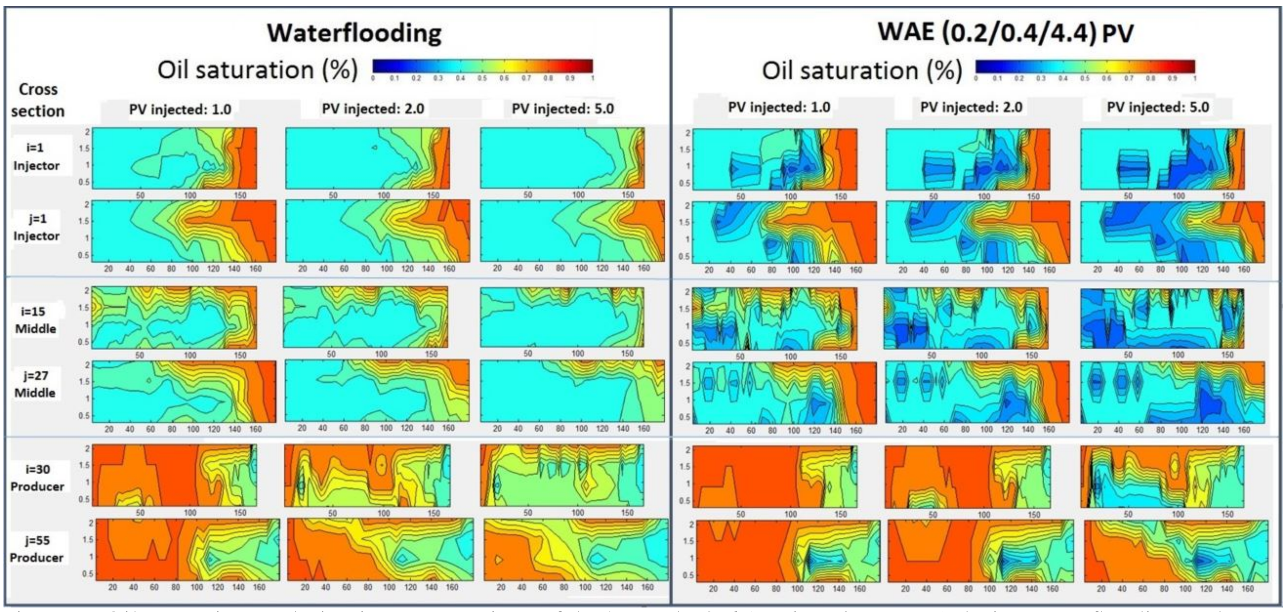

Figure 7: Oil saturation evolution in cross-sections of the layers k=3-6 (*Tarbert formation*) during waterflooding and WAE injection of (0.2/0.4/4.4) PV.

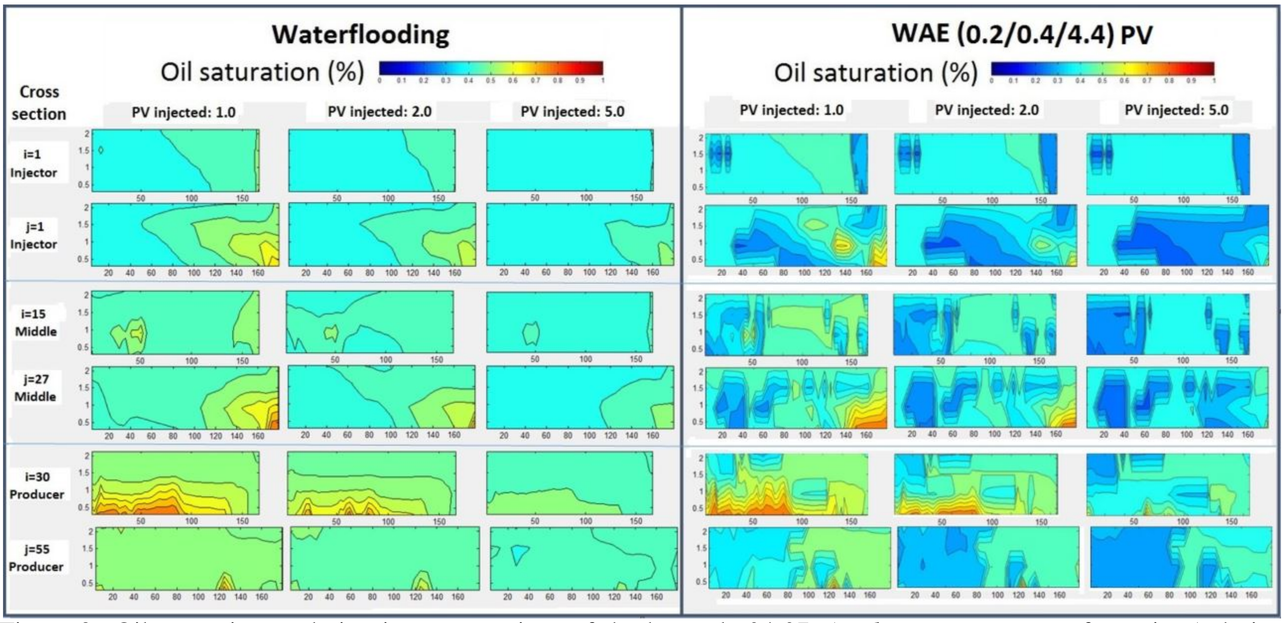

Figure 8: Oil saturation evolution in cross-sections of the layers k=34-37, (*Tarbert - Upper Ness* formations) during waterflooding and WAE injection of (0.2/0.4/4.4) PV.

Effect of the emulsion bench size is shown in Fig. 9(a)-(b). ORF is evaluated for both group of layers after WAE injection with emulsion bench sizes of 0.2, 0.4 and 1.2 PV. Results show in Fig. 9(a) that, independently of the injection process, higher oil recoveries are reached in the *Tarbert-Upper Ness* layers. WAE cases produced extra oil recovery in comparison with waterflooding but differently from that observed in 2D simulations (Fig. 3(a)), increase of the emulsion bench size did not caused a significant impact in oil recovery. Higher injector pressure and reduction in WCUT is observed in Fig. 9(b) for the *Tarbert-Upper Ness* layers during waterflooding and WAE injections, which may be associated to the residual oil mobilization.

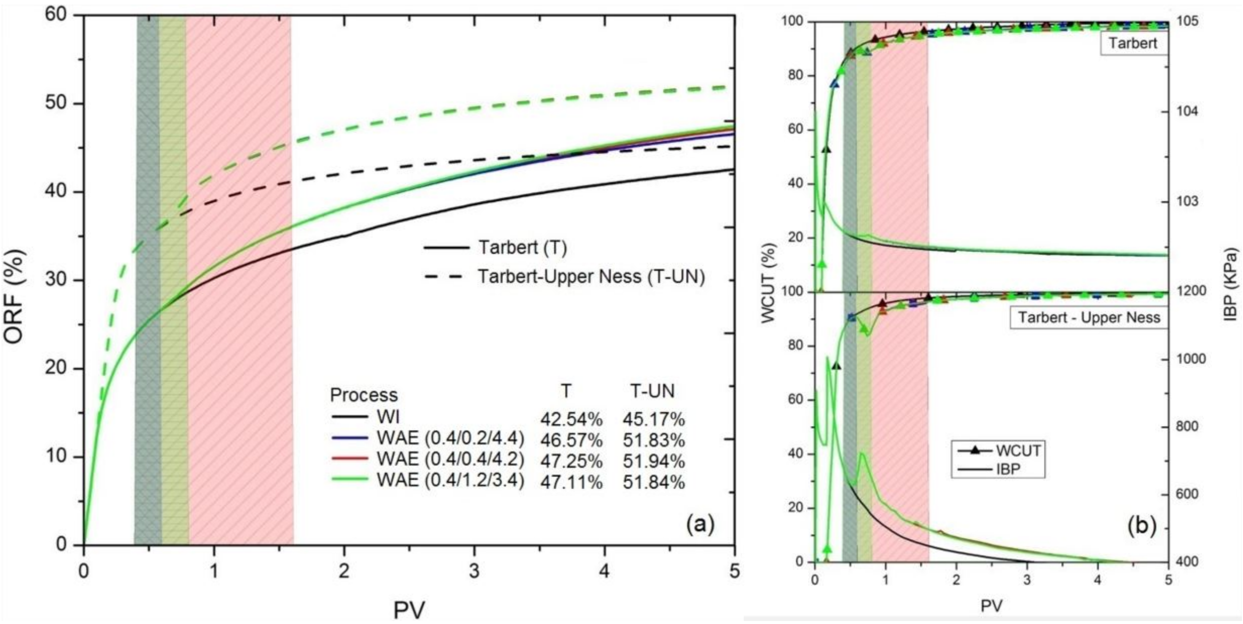

Figure 9: Effect of the injected emulsion bench size in both group of layers.

4. CONCLUSIONS

In this work gravitational forces were added to a two-phase flow model that considered capillary and drop concentration effects during macroemulsion flow. 2D simulations results of WAE injection in a highly heterogeneous reservoir highlight the impact of capillary number on the emulsion performance, so appropriate design of emulsions is key to the success of WAE injection. Water cut oscillations and injection pressure response typically observed during WAE injection was reproduced by the model. 2D and 3D simulations showed that early emulsion injection accelerates oil production even in highly heterogeneous reservoirs, but increasing emulsion bench size in WAE processes may not necessarily increase oil recovery. An enhanced oil displacement efficiency and large vertical sweep efficiency observed in 3D simulations after WAE injection suggest that emulsion benefits may be exploited successfully in heterogeneous and stratified reservoirs. Further work is needed to incorporate effects of capillary trapping and drop to pore size distribution in the model as well as experimental relative permeability to evaluate emulsion features and capillary number effects.

5. ACKNOWLEDGEMENTS

The authors would like to acknowledge Petrobras for financial support.

6. REFERENCES

Aarnes, J.E., Gimse, T. and Lie, K.A., 2007. “An introduction to the numerics of flow in porous media using matlab”. In *Geometric modelling, numerical simulation, and optimization: applied mathematics at SINTEF*, Springer Berlin Heidelberg, pp. 265–306.

Alvarado, D.A. and Marsden, S.S., 1979. “Flow of oil-in-water emulsion through tubes and porous media”. *SPE Journal*, Vol. 19, pp. 369–377".

Cobos, S., Carvalho, M.S. and Alvarado, V., 2009. “Flow of oil-water emulsions through a constricted capillary”. *International Journal of Multiphase Flow*, Vol. 35, pp. 507–515.

Corey, A.T., 1954. “The interrelation between gas and oil relative permeabilities”. *Producer Monthly*, Vol. 19, pp. 38–41.

Engelke, B., Carvalho, M.S. and Alvarado, V., 2013. “Conceptual darcy-scale model of oil displacement with macroemulsion”. *Energy & Fuels*, Vol. 27, pp. 1967–1973.

Guillen, V.R., Carvalho, M.S. and Alvarado, V., 2012a. “Pore scale and macroscopic displacement mechanism in emulsion flooding”. *Transport in Porous Media*, Vol. 94, pp. 197–206.

Guillen, V.R., Romero, M.I., Carvalho, M.S. and Alvarado, V., 2012b. “Capillary-driven mobility control in macro emulsion flow in porous media”. *International Journal of Multiphase Flow*, Vol. 43, pp. 62–65.

McAuliffe, C.D., 1973. “Crude-oil-in-water emulsions to improve fluid-flow in an oil reservoir”. *Journal of Petroleum Technology*, Vol. 25, pp. 721–726.

Ponce, F.R.V., Carvalho, M.S. and Alvarado, V., 2014. “Oil recovery modeling of macro-emulsion flooding at low capillary number”. *Journal of Petroleum Sciences and Technology*, Vol. 119, pp. 112–122.

Ponce, F.R.V., Carvalho, M.S. and Alvarado, V., 2017. “Water-alternating-macroemulsion reservoir simulation through capillary number-dependent modeling”. *Journal of the Brazilian Society of Mechanical Sciences and Engineering*. doi:http://link.springer.com/article/10.1007/s40430-017-0885-7.

Romero, M.I., Carvalho, M.S. and Alvarado, V., 2011. “Experiments and network model of flow of oil-water emulsion in porous media”. *Physical Review E*, Vol. 84, p. 046305.

Society of Petroleum Engineering, 2009. “SPE Comparative Solution Project - description of model 2”. Online `http://www.spe.org/web/csp/datasets/set02.htm`. Accessed: 2016-06-12.

7. RESPONSIBILITY NOTICE